Adhesive and Nonadhesive, Large Strain AFM Indentation of Rubber-like Materials

David C. Lin[1], Emilios K. Dimitriadis[2], and Ferenc K. Horkay[1]
[1]Laboratory of Integrative and Medical Biophysics, National Institutes of Health, Bethesda, MD, 20892
[2]National Institute of Biomedical Imaging and Bioengineering, National Institutes of Health, Bethesda, MD, 20892

ABSTRACT

Atomic force microscopy is an established technique for probing the local elastic properties of materials at submicron scales. In some cases, linear elastic contact theories based on Hertzian and adhesive contact mechanics suffice to model the indentation process. However, at the large strains that are common in many nanoindentation experiments, the linear models become invalid. A force-indentation relationship based on the Mooney-Rivlin equation and capable of being extended to adhesive behavior that closely follows the Derjaguin-Muller-Toporov (DMT) theory is presented. We use this new relationship to fit data from the AFM indentation of highly swollen, chemically crosslinked poly(vinyl alcohol) gels, which are known to exhibit rubber elastic behavior. The extracted Young's moduli agree well with values obtained from macroscopic uniaxial compression tests.

INTRODUCTION

The well-established field of indentation, including the theories used to model the mechanics of contact between the indenter and the probed material, has experienced rapid advancement with the advent of instrumented nanoindentation [1,2]. The prevalent nanoindentation technologies (atomic force microscopy – AFM, and depth-sensing nanoindentation) permit the mechanical probing of surfaces at submicron length scales. Although linear elastic models based on the Hertz theory [3] can be applied successfully [4], tip-sample interactions (primarily adhesion) can cause the indentation behavior to deviate significantly from that predicted by the models. Adhesive theories, also predicated on linear elasticity, have therefore been developed by Johnson *et al* (JKR theory) [5], Derjaguin *et al* (DMT theory) [6], and Maugis (Maugis-Dugdale, or MD theory) [7].

In nanoindentation, deformation of the indented material beyond the linear elastic limit can be unavoidable depending on the geometry of the indenter. Although spherical tips generate much smaller stresses and strains than common tapered tips at comparable depths [8], a combination of small tip diameter and narrow range of linearity may still limit the linear regime to indentation depths that fall outside the resolution of the instrument. Even when it is feasible to either restrict the maximum indentation depth or truncate the dataset, accuracy may be adversely affected by signal-to-noise ratios that are typically higher in the vicinity of tip-sample contact than at larger indentation depths. Here, we are interested in the nanoindentation of materials that exhibit rubber-like behavior. These materials can be elastically deformed to large strains, with the stress-strain relationship generally adhering to the Mooney-Rivlin model; at small strains, the relationship is approximately linear.

In this paper, we make use of an automated algorithm we previously described [4] based on Pietrement and Troyon's empirical formulation of the MD theory [9] and present an approximate

Mooney-Rivlin force-indentation relationship for spherical indenters based on the Hertz and DMT theories. Results of AFM indentation experiments performed on chemically crosslinked poly(vinyl alcohol) gels, which have been shown to obey rubber elasticity [10] are also presented.

THEORY

The JKR and DMT theories for indentation with a spherical tip are applicable to opposite extremes of the relationship between material compliance, strength of the tip-sample adhesive force, and tip radius [11]. The JKR theory is valid for relatively compliant materials that adhere strongly to tips with large radii whereas the DMT theory applies to the indentation of stiffer materials with small tips and weak adhesive interactions. In the intermediate regime, the mechanics can be modeled using the MD theory and its empirical forms [9,12]. Details of the specific theories can be found in the original references [5-7,9,12].

To formulate an adhesive contact model based on rubber elasticity, we start by defining the average indentation stress (σ^*) and strain (ε^*) as

$$\sigma^* = F / \pi a^2 \tag{1}$$

$$\varepsilon^* = a / R \tag{2}$$

where F is the net indentation force, a is the contact radius, and R is the radius of the spherical indenter. The classical Hertz equation and the DMT theory relating F to the indentation depth δ is

$$F = F_n + F_{ad} = \frac{4 E R^{1/2} \delta^{3/2}}{3(1 - v^2)} \tag{3}$$

where $\delta = a^2/R$ and E and v are Young's modulus and Poisson's ratio of the indented material, respectively. Note that $F_{ad} = 0$ in the Hertz theory and that the ratio of σ^* to ε^* is a constant, as expected for linear elastic indentation. The nonlinear Mooney-Rivlin relationship between stress σ and the stretch ratio λ for an incompressible material can be expressed as [13]

$$\sigma = C_1 [\lambda - \lambda^{-2}] + C_2 [1 - \lambda^{-3}] \tag{4}$$

where C_1 and C_2 are constants. Adopting the convention that σ^* and ε^* are positive for $\delta > 0$ (note that since indentation is predominantly a compressive process, this convention is contrary to the standard engineering notation used in the Mooney-Rivlin equation), Equation (4) can be rewritten with σ replaced by $-\sigma^*$ and λ by $(1 - \varepsilon^*)$. Substituting Equations 1 and 2 into the recast Equation 4 and assuming that the relationship between a and δ at large strain changes negligibly from that at small strains ($a = R^{1/2}\delta^{1/2}$), the following force-indentation relationship is obtained:

$$F = \pi R^{1/2} C_1 \left(\frac{\delta^{5/2} - 3R^{1/2}\delta^2 + 3R\delta^{3/2}}{\delta - 2R^{1/2}\delta^{1/2} + R} \right) + \pi R^{1/2} C_2 \left(\frac{R^{1/2}\delta^{5/2} - 3R\delta^2 + 3R^{3/2}\delta^{3/2}}{-\delta^{3/2} + 3R^{1/2}\delta - 3R\delta^{1/2} + R^{3/2}} \right) \tag{5}$$

Note that the sum of C_1 and C_2 are related to the material properties by

$$C_1 + C_2 = \frac{4E_0}{9\pi(1-\nu^2)} \qquad (6)$$

where E_0 is the initial Young's modulus.

   The applied force and resulting indentation are measured indirectly in the AFM, with the former inferred from the deflection of the cantilever and the latter depending on both cantilever deflection and the displacement of the cantilever base. Hence, conversion of acquired values of cantilever deflection (d) and base displacement (z) relies on the identification of the reference points listed in Table I [4]. In the case of adhesion, the applied force is nonzero at the point of contact or separation because it must balance the adhesive force; the zero force reference occurs at some positive indentation depth. Once the reference points have been identified, the adhesive force is

$$F_{ad} = -k(d_0 - d_1) = 2\pi\gamma R \qquad (7)$$

where k is the spring constant of the cantilever and γ is the interfacial energy in units of energy per unit area [6,9].

Table I. Essential reference points and their relation to force and indentation.

Non-adhesive (Hertz)	Contact: (z_0,d_0)	$F_n = k(d - d_0)$ $\delta = z - z_0 - (d - d_0)$	k: spring constant of cantilever
Adhesive (DMT)	Contact: (z_0,d_0) Zero force: (z_1,d_1)	$F_n = k(d - d_1)$ $\delta = z - z_0 - (d - d_0)$	

EXPERIMENT

   Poly(vinyl alcohol) of MW ($= 70,000 - 100,000$) was obtained from Sigma (St. Louis, MO) and dissolved in water at 99 °C to form a 14% stock solution. Gels at polymer concentrations of 6% and 12% were made by crosslinking the polymer in aqueous solution with glutaraldehyde at pH ~ 1.5. The ratio of units of crosslinker to units of monomer was maintained at 1:100. Gel cylinders (1 cm diameter, 1 cm height) and films (> 2 mm thick) were cast for macroscopic displacement-controlled compression testing and AFM nanoindentation, respectively. The samples were swollen to equilibrium in water prior to testing. General purpose silicon nitride tips (Veeco, Santa Barbara, CA) with 9.6 μm polystyrene or 5.5 μm glass beads attached were used for the AFM measurements, performed using a commercial AFM (Bioscope I with Nanoscope IIIA controller, Veeco). The spring constant of the cantilever was measured by the thermal tune method while bead diameters were measured from images acquired during the attachment process. Accuracy of the cantilever deflections was ascertained by measuring the sensitivity against a rigid surface prior to testing. A raster scanning approach ("force-volume") was applied to automatically perform indentations, typically set to a resolution of 16×16 (256

total indentations) over an area of 50×50 µm. Further details of the procedure and results of the nanoindentation experiments using Equation 3 and the empirical Pietrement-Troyon equation have been reported elsewhere [4]. Here, we apply nonlinear analysis to the same datasets and compare the results (extracted values of Young's modulus) to those obtained using the linear theories. All analysis was conducted using software developed in MATLAB (Mathworks, Natick, MA) and based on the algorithms described elsewhere [4].

DISCUSSION

Maugis introduced a nondimensional parameter to delimit the transition region between the opposing JKR and DMT theories. The empirical forms of the MD theory developed by Carpick *et al* and by Pietrement and Troyon make use of an equivalent parameter, α, where $\alpha = 1$ corresponds to the JKR case and $\alpha = 0$ to the DMT theory. It is important to note that Equation 5 is not valid when α deviates from the DMT limit because the relationship between σ^* and ε^* is not linear in the JKR and empirical MD models even at small strains. In applying Pietrement and Troyon's equation to the indentation of poly(vinyl alcohol) gels, we found the samples to be close to the DMT limit of the adhesion spectrum, with $\alpha = 0$ in the majority of cases [4]. Results are presented in Table II. Adhesion was evident only in the retraction strokes, prior to tip-sample separation. The small strain analysis of the AFM data was performed by truncating the datasets at about 15% strain and applying either the Hertz equation (extension stroke) or the Pietrement-Troyon equation (retraction stroke) [4]. The large strain analysis was performed without truncation and fitting Equation 5 with $F_{ad} = 0$ (extension stroke) or with F_{ad} determined from the identified contact point (retraction stroke). The gels were assumed to be incompressible ($\nu = 0.5$) in all cases. The generally good agreement between macroscopic compression and AFM indentation can be seen from the summary of results found in Table II.

The Mooney-Rivlin model is derived from a phenomenological treatment of large strain elasticity. Although many refinements to the theory have been formulated [13], the model still provides acceptable fits of many sets of experimental data. We chose it as the basis for modeling indentation mechanics because of its relative simplicity. Figure 1 shows an example of Equation 5 fit to the extension and retraction portions of a typical dataset from the indentation of the 6% gel. Also shown are the resulting fits when the linear elastic equations are applied to a smaller range of indentation strain (~15%). The errors in the Mooney-Rivlin fits are consistently small even to the maximum indentation strain, indicating the rubber elastic nature of the deformation. Table II shows that similar values of Young's modulus were obtained from both methods. Although not the case in this experiment, errors associated with the linear models can be significantly higher due to greater contribution from noise in the vicinity of the contact point. It is therefore advantageous to apply models that allow inclusion of the full dataset in the analysis.

Table II. Young's moduli from compression and AFM nanoindentation (mean ± SD).

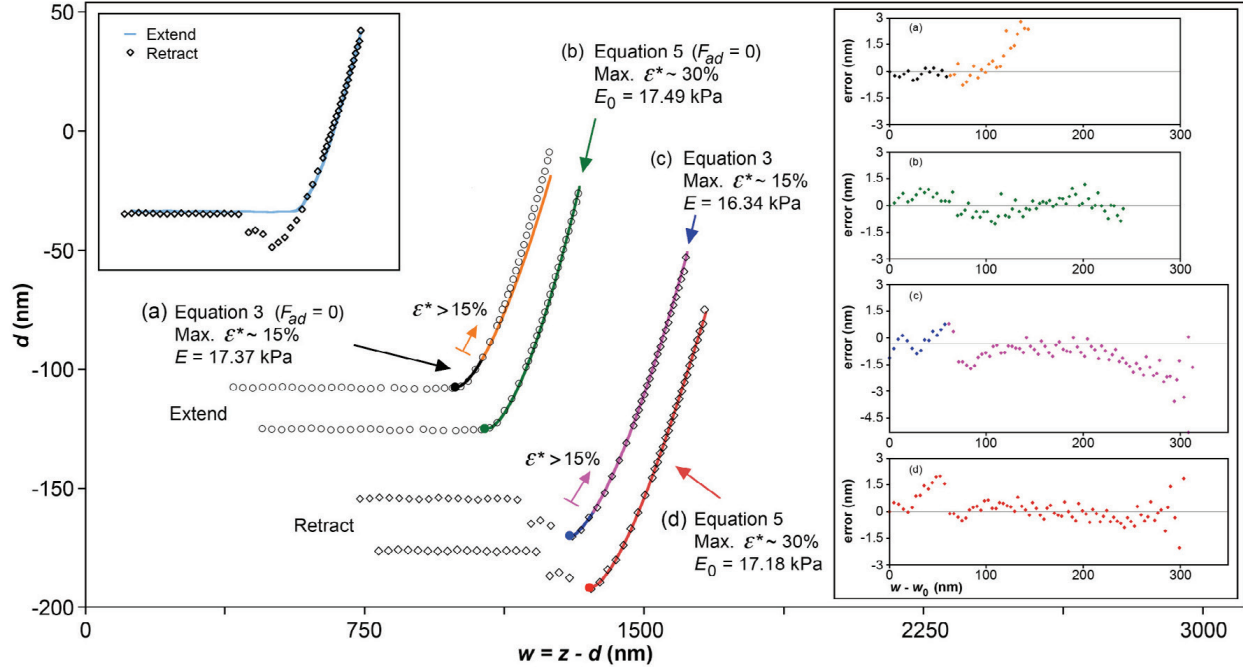| %	Macro. (kPa)	Small Strain, Linear Elastic		Large Strain, Mooney-Rivlin	
		Extend (kPa)	Retract (kPa)	Extend (kPa)	Retract (kPa)
6	21.51 ± 0.59	16.55 ± 2.74	19.39 ± 3.26	18.23 ± 2.38	19.51 ± 4.69
12	115.50 ± 1.86	113.66 ± 6.06	108.98 ± 9.17	115.82 ± 7.21	110.08 ± 13.17

Figure 1. Fits of a sample dataset from indentation of the 6% gel using both linear elastic (Equation 3) and Mooney-Rivlin (Equation 5) contact models. Every fifth point of the raw data is plotted. Contact points are indicated by solid dots, with coordinates (w_0, d_0). For display purposes, the curves are shifted apart. For the small strain analysis, fits are extended beyond the imposed strain limit for comparison with the Mooney-Rivlin fits. The tip extension curve has no apparent adhesive interactions while the first release point is taken to be the contact point in the retraction curve. The equation used for each particular fit is indicated along with the strain cutoff and the extracted Young's modulus. Right inset shows point-by-point plot of errors (difference between predicted d and actual d) for each fit. Left inset shows extension and retraction curves plotted on the same scale for comparison.

The existence of tip-sample adhesion is demonstrated by the conspicuous valley in the d-w retraction curve in Figure 1. It is clear that the adhesive force can be determined independently of the contact model applied. The neutrality of the poly(vinyl alcohol) gels in our experiments prevented divergent adhesive behavior from point to point. In samples with highly inhomogeneous surface energy profiles, AFM probing can in principle, be employed to map changes in the interfacial energy.

The assumption of a Hertzian contact radius over the range of indentation depths is significant to the derivation of the force-indentation relationship represented by Equation 5. Numerical analysis of the errors associated with this assumption has yet to be performed. However, studies on the indentation of plastic materials may provide some insight into the validity of the assumption. It has been shown that the contact radius of materials undergoing plastic deformation differs from the Hertzian form by a constant factor [14] and the Hertzian contact radius was found to extend beyond the yield point of the material [15]. Based on these numerical studies of plastic indentation and the good agreement between the AFM and

macroscopic compression data, we believe that the assumption for rubber elastic materials is a valid first approximation.

CONCLUSIONS

The prevalence of nanoindentation in measuring the local elastic properties of a wide range of materials necessitates the development of contact models that accurately represent various material behaviors. Simple force-indentation relationships are especially desirable for automated and high-throughput applications. The approximate Mooney-Rivlin equation introduced here satisfies this requirement and appears capable of modeling the indentation of rubber-like materials, both with and without the influence of adhesive interactions. The approach used to derive the equation can also be applied to other hyperelastic models (e.g., neo-Hookean and polynomial forms).

ACKNOWLEDGMENTS

REFERENCES

1. S.A. Syed Asif, R.J. Colton, K.J. Wahl, in *Interfacial Properties on the Submicrometer Scale*, edited by J. Frommer and R.M. Overney (ACS/Oxford University Press, Washington, D.C., 2001), pp.198-215.
2. M.R. VanLandingham, J. Res. Natl. Inst. Stand. Technol. **108**, 249 (2003).
3. H. Hertz, J. Reine Agnew. Math. **5**, 12 (1881).
4. D.C. Lin, E.K. Dimitriadis, F. Horkay, J. Biomech. Eng. **129**, 430 (2007; Part II in press).
5. K.L. Johnson, Proc. R. Soc. Lond. A **324**, 301 (1971).
6. B.V. Derjaguin, V.M. Muller, Y.P. Toporov, J. Colloid Interface Sci. **53**, 314 (1975).
7. D. Maugis, J. Colloid Interface Sci. **150**, 243 (1992).
8. E.K. Dimitriadis, F. Horkay, J. Maresca, B. Kachar, R.S. Chadwick, Biophys. J. **82**, 2798 (2002).
9. O. Pietrement, M. Troyon, J. Colloid Interface Sci. **226**, 166 (2000).
10. F. Horkay, M. Nagy, Polymer Bull. **3**, 457 (1980).
11. D. Tabor, J. Colloid Interface Sci. **58**, 2 (1976).
12. R.W. Carpick, D.F. Ogletree, M. Salmeron, J. Colloid Interface Sci. **211**, 395 (1999).
13. L.R.G. Treloar, *The Physics of Rubber Elasticity*, 3rd ed (Oxford University Press, Oxford, 1975).
14. A.F. Bower, N.A. Fleck, A. Needleman, N. Ogbonna, Proc. R. Soc. Lond. A **441**, 97 (1993).
15. S.D. Mesarovic, N.A. Fleck, Proc. R. Soc. Lond. A **455**, 2707 (1999).